

Accepted Manuscript

Synthesis and evaluation of the cytotoxic activity of Furanaphthoquinones tethered to 1*H*-1,2,3-triazoles in Caco-2, Calu-3, MDA-MB231 cells

Dora C.S. Costa, Gabriella Silva de Almeida, Vitor Won-Held Rabelo, Lucio Mendes Cabral, Plínio Cunha Sathler, Paula Alvarez Abreu, Vitor Francisco Ferreira, Luiz Cláudio Rodrigues Pereira da Silva, Fernando de C. da Silva

PII: S0223-5234(18)30574-9

DOI: [10.1016/j.ejmech.2018.07.018](https://doi.org/10.1016/j.ejmech.2018.07.018)

Reference: EJMECH 10553

To appear in: *European Journal of Medicinal Chemistry*

Received Date: 16 May 2018

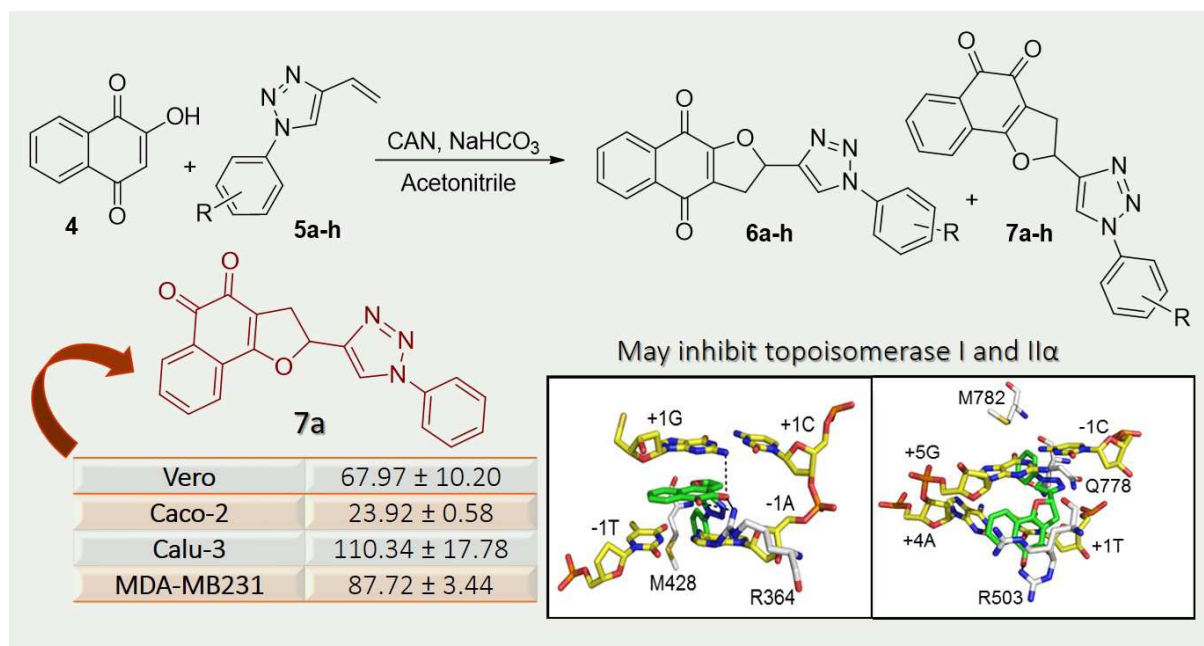
Revised Date: 28 June 2018

Accepted Date: 7 July 2018

Please cite this article as: D.C.S. Costa, G.S. de Almeida, V.W.-H. Rabelo, L.M. Cabral, Plí.Cunha. Sathler, P. Alvarez Abreu, V.F. Ferreira, L. Cláudio Rodrigues Pereira da Silva, F.d.C. da Silva, Synthesis and evaluation of the cytotoxic activity of Furanaphthoquinones tethered to 1*H*-1,2,3-triazoles in Caco-2, Calu-3, MDA-MB231 cells, *European Journal of Medicinal Chemistry* (2018), doi: 10.1016/j.ejmech.2018.07.018.

This is a PDF file of an unedited manuscript that has been accepted for publication. As a service to our customers we are providing this early version of the manuscript. The manuscript will undergo copyediting, typesetting, and review of the resulting proof before it is published in its final form. Please note that during the production process errors may be discovered which could affect the content, and all legal disclaimers that apply to the journal pertain.





Synthesis and Evaluation of the Cytotoxic Activity of Furanaphthoquinones Tethered to 1*H*-1,2,3-Triazoles in Caco-2, Calu-3, MDA-MB231 Cells

Dora C. S. Costa,^a Gabriella Silva de Almeida,^b Vitor Won-Held Rabelo,^c Lucio
Mendes Cabral,^b Plínio Cunha Sathler,^b Paula Alvarez Abreu,^c Vitor Francisco
Ferreira,^{d,*} Luiz Cláudio Rodrigues Pereira da Silva,^{b,*} Fernando de C. da Silva^{a,*}

^a Universidade Federal Fluminense, Departamento de Química Orgânica, Instituto de Química, Campus do Valonguinho, Niterói, RJ, CEP 24020-150, Brazil.

^b Universidade Federal do Rio de Janeiro, Laboratório de Tecnologia Industrial Farmacêutica (LabTIF), Faculdade de Farmácia, Rio de Janeiro, RJ, CEP 21941-902, Brazil.

^c Universidade Federal do Rio de Janeiro, Laboratório de Modelagem Molecular e Pesquisa em Ciências Farmacêuticas (LaMCiFar), NUPEM, Campus Macaé, RJ, CEP 27965-045, Brazil.

^d Universidade Federal Fluminense, Departamento de Tecnologia Farmacêutica, Faculdade de Farmácia, Niterói, RJ, CEP 24241-002, Brazil.

Corresponding authors

Biological Assays: Luiz Cláudio Rodrigues Pereira da Silva, Universidade Federal do Rio de Janeiro, Laboratório de Tecnologia Industrial Farmacêutica (LabTIF), Faculdade de Farmácia, Rio de Janeiro, RJ, 21941-902, Brazil; E-mail: luizclaudio@pharma.ufrj.br

Chemistry: Fernando de Carvalho da Silva, Universidade Federal Fluminense, Departamento de Química Orgânica, Instituto de Química, Campus do Valonguinho, CEP 24020-150, Niterói-RJ, Brazil; E-mail: gqoferando@vm.uff.br

Vitor Francisco Ferreira, Universidade Federal Fluminense, Departamento de Tecnologia Farmacêutica, Faculdade de Farmácia, Niterói, RJ, CEP 24241-002, Brazil. vitorferreira@id.uff.br

Abstract: Napthoquinones and 1,2,3-triazoles are structural pharmacophore that is known to impart several cancer cells. This work shows a synthetic methodology to obtain hybrid molecules involving naphthoquinone and triazol scaffold as multiple ligands. A simple and efficient synthetic route was used to prepare a series of sixteen compounds being eight 2-(1-aryl-1*H*-1,2,3-triazol-4-yl)-2,3-dihydronaphtho[1,2-*b*]furan-4,5-diones and eight 2-(1-aryl-1*H*-1,2,3-triazol-4-yl)-2,3-dihydronaphtho[2,3-*b*]furan-4,9-diones. These compounds were tested in MDA-MB231, Caco-2 and Calu-3 human cancer cells, and among them **7a** was the most selective compound on Caco-2 cells, the most sensitized cell line in this study. In silico study suggest that the blockage of topoisomerase I and II α may be one of the mechanisms of action responsible for the cytotoxic effect of **7a** in Caco-2 cells.

Keywords: quinones; triazole; cancer; anticancer agents; molecular modelling; topoisomerase.

1. Introduction

There are several synthetic and natural low molecular weight naphthoquinones with many applications in various scientific and technological fields [1]. In this sense, quinones have already been described with a diversity of bioactivities such as anticancer [1], molluscicides [2,3], antiparasitics [4-6], antimalarial [7], leishmanicides [8], anti-inflammatory [9], antifungal [10], antimicrobial [11] and trypanocidal [12].

On the other hand, heterocyclic rings are considered the pillars of medicinal chemistry because they are incorporated in the molecular structure of most of the drugs available in the market. From the earliest days of medicinal chemistry, these rings were known to be the pharmacophore in many compounds with biological activities. Taylor and colleagues estimated that about six new ring systems are created per year and some of them are incorporated into new drugs. According to those authors, 1,2,4 and 1,2,3-triazoles are among the 100 most commonly used ring systems in small molecules listed in the FDA orange book [13].

Although the scaffold quinones and 1,2,3-triazoles are of major importance separately, molecules containing these two nuclei only have been studied in recent years against various diseases showing that this molecular combination have great potential synergism, i.e., are more bioactive when coupled than in the isolated form (*e.g.* the naphthoquinone-1,2,3-triazole conjugates **1** [14] and **2** [15] with good antitumor activity).

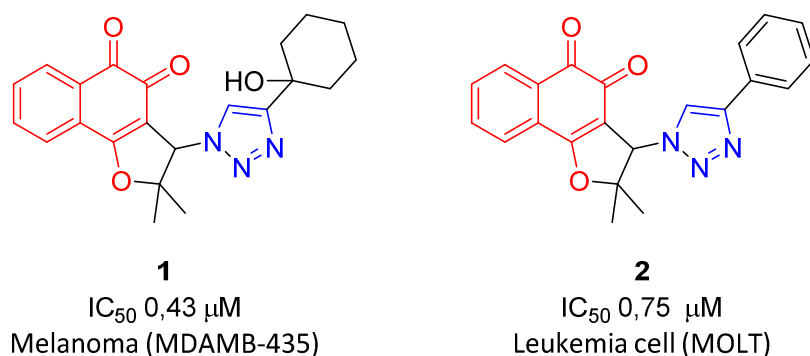


Fig. 1. Examples of hybrids naphthoquinone-1,2,3-triazole with high activities in cancer cells

As part of our research program on the synthesis of biologically active quinones, we became interested in the synthesis and antitumor evaluation of hybrids naphthoquinone-1,2,3-triazoles. Among the aforementioned hybrids, a series of eight 2-(1-phenyl-1*H*-1,2,3-triazol-4-yl)-2,3-dihydronaphtho[1,2-*b*]furan-4,5-dione (**6a-h**) and eight 2-(1-phenyl-1*H*-1,2,3-triazol-4-yl)-2,3-dihydronaphtho[2,3-*b*]furan-4,9-dione (**7a-h**) were synthesized and screened *in vitro* against MDA-MB231, Caco-2 and Calu-3 human cancer cell lines and also evaluated their cell viability on Vero cells.

2. Experimental Section

2.1. Chemistry

The reagents were purchased from Sigma-Aldrich Brazil and were used without further purification. Column chromatography was performed with silica gel 60 (Merck 70-230 mesh). Analytical thin layer chromatography was performed with silica gel plates (Merck, TLC silica gel 60 F₂₅₄), and the plates were visualized using UV light. The indicated yields refer to homogeneous materials purified by chromatography and

confirmed by spectroscopic techniques. Melting points were obtained on a Thermo scientific 9100 apparatus and were uncorrected. Infrared spectra were collected using KBr pellets on a Perkin-Elmer model 1420 FT-IR spectrophotometer, and the spectra were calibrated relative to the 1601.8 cm^{-1} absorbance of polystyrene. ^1H and ^{13}C NMR were recorded at room temperature using a Varian Mercury 300 or Varian Mercury 400 MHz, in the DMSO-d_6 . Chemical shifts (δ) are given in ppm and coupling constants (J) in Hertz. The chemical shift data were reported in units of δ (ppm) downfield from solvent, and the solvent was used as an internal standard; coupling constants (J) are reported in hertz and refer to apparent peak multiplicities. High-resolution mass spectra (HRMS) were recorded on a MICROMASS Q-TOF mass spectrometer (Waters).

2.1.1. General procedure for the preparation of **4a-h** and **5a-h**

To a stirred suspension of 2-hydroxy-1,4-naphthoquinone **5** (1.3 mmol, 1.0 eqv.) in freshly dried acetonitrile, 0.48 g of NaHCO_3 was added at once, in an ice bath and sodium chloride at 0-5 °C. This mixture was stirred for 15 min. and then the appropriate 4-vinyl-1*H*-1,2,3-triazoles **4** (1.1 equiv.) was added at once, at the same temperature. After that, 1.75 g of ceric ammonium nitrate (CAN) was added slowly and reaction mixture was stirred until total consumption of the starting material. During the reaction time, it was allowed that the bath temperature rose up spontaneously to room temperature. The acetonitrile was removed under reduced pressure and the resulting crude was purified *via* silica flash chromatography, using a gradient mixture of chloroform/ethyl acetate, as eluent to obtain 1,4-isomer **6a-h** as a yellow solid and the 1,2-isomer **7a-h** as an orange solid.

2.1.1.1. 2-(1-phenyl-1H-1,2,3-triazol-4-yl)-2,3-dihydronaphtho[2,3-b]furan-4,9-dione (**6a**). Yellow solid. m.p. 219-220 °C. IR (KBr, cm⁻¹): ν 1681, 1624 (C-H Ar), 1593, 1503, 1389, 1241, 1200, 1056, 956, 832, 757, 718, 685. ¹H NMR (DMSO-d₆, 500 MHz) δ ppm: 3.53 (dd, *J* 17.0 and 8.0 Hz, 1H), 3.66 (dd, *J* 17.0 and 10.8 Hz, 1H), 6.32 (dd, *J* 10.8 and 8.0 Hz, 1H), 7.51 (t, *J* 7.5 Hz, 1H), 7.61 (t, *J* 8.0 Hz, 2H), 7.81-7.89 (m, 2H), 7.90 (d, *J* 7.5 Hz, 2H), 8.05-7.97 (m, 2H), 9.09 (s, 1H). ¹³C NMR (DMSO-d₆, 125 MHz APT) δ ppm: 32.7, 79.0, 120.7, 123.1, 124.5, 126.0, 126.3, 129.3, 130.3, 131.8, 133.0, 133.8, 134.9, 137.0, 146.9, 159.3, 177.6, 182.0. HRMS-ESI *m/z* [M + H]⁺ calcd for C₂₀H₁₄N₃O₃: 344.10297; found: 344.10297. Δ = 0 ppm.

2.1.1.2. 2-(1-phenyl-1H-1,2,3-triazol-4-yl)-2,3-dihydronaphtho[1,2-b]furan-4,5-dione (**7a**). Orange solid. m.p. 208-209 °C. IR (KBr, cm⁻¹): ν 1697, 1650, 1614, 1571, 1489, 1274, 1250, 1219, 853, 755, 723, 687. ¹H NMR (DMSO-d₆, 500 MHz) δ ppm: 3.41 (dd, *J* 15.4 and 7.5 Hz, 1H), 3.54 (dd, *J* 15.4 and 10.2 Hz, 1H), 6.44 (dd, *J* 10.2 and 7.5 Hz, 1H), 7.50-7.53 (m, 1H), 7.60-7.65 (m, 3H), 7.69 (td, *J* 7.8 and 1.1 Hz, 1H), 7.77 (td, *J* 7.8 and 1.1 Hz, 1H), 7.93-7.88 (m, 2H), 7.98 (dd, *J* 7.8 and 1.1 Hz, 1H), 9.12 (s, 1H). ¹³C NMR (DMSO-d₆, 125 MHz APT) δ ppm: 31.5, 79.9, 115.0, 120.1, 122.5, 124.2, 126.8, 128.6, 128.8, 129.8, 130.5, 132.0, 134.6, 136.4, 146.4, 167.4, 174.8, 180.3. HRMS-ESI *m/z* [M + H]⁺ calcd for C₂₀H₁₄N₃O₃: 344.10297; found: 344.10297. Δ = 0 ppm.

2.1.1.3. 2-(1-(4-tolyl)-1H-1,2,3-triazol-4-yl)-2,3-dihydronaphtho[2,3-b]furan-4,9-dione (**6b**). Yellow solid. m.p. 254-255 °C. IR (KBr, cm⁻¹): ν 1679, 1622, 1585, 1520, 1389, 1389, 1238, 1189, 1055, 955, 855, 815, 720, 620. ¹H NMR (DMSO-d₆, 500 MHz) δ ppm: 2.38 (s, 3H), 3.52 (dd, *J* 17.0 and 7.9 Hz, 1H), 3.65 (dd, *J* 17.0 and 10.9 Hz, 1H), 6.31 (dd, *J* 10.9 and 7.9 Hz, 1H), 7.40 (d, *J* 8.5 Hz, 1H), 7.77 (d, *J* 8.5 Hz, 2H), 7.80-

7.88 (m, 2H), 7.99-8.03 (m, 2H), 9.03 (s, 1H). ^{13}C NMR (DMSO- d_6 , 125 MHz APT) δ ppm: 20.4, 32.1, 78.5, 120.0, 122.4, 123.9, 125.4, 125.7, 130.1, 131.2, 134.2, 133.3, 134.3, 138.5, 146.3, 158.7, 177.0, 181.4. HRMS-ESI m/z $[\text{M} + \text{H}]^+$ calcd for $\text{C}_{21}\text{H}_{16}\text{N}_3\text{O}_3$: 358.11862; found: 358.11862. $\Delta = 0$ ppm.

2.1.1.4. 2-(1-(*p*-tolyl)-1*H*-1,2,3-triazol-4-yl)-2,3-dihydronaphtho[1,2-*b*]furan-4,5-dione (**7b**). Orange solid, m.p.: 239-240 °C. IR (KBr, cm^{-1}): ν 1694, 1646, 1613, 1570, 1517, 1486, 1345, 1255, 1211, 1143, 1076, 996, 972, 876, 816, 771, 725, 703, 660. ^1H NMR (DMSO- d_6 , 500 MHz) δ ppm: 3.38 (s, 3H), 3.40 (dd, J 15.3 and 7.5 Hz, 1H), 3.53 (dd, J 15.3 and 10.5 Hz, 1H), 6.43 (dd, J 10.5 and 7.5 Hz, 1H), 7.40 (d, J 8.3 Hz, 2H), 7.62-7.74 (m, 3H), 7.79 (d, J 8.3 Hz, 2H), 7.97 (dd, J 8.0 and 1.0 Hz, 1H) 9.07 (s, 1H). ^{13}C NMR (DMSO- d_6 , 125 MHz APT) δ ppm: 21.0, 32.1, 80.5, 115.6, 120.6, 122.9, 124.8, 127.4, 129.2, 130.7, 131.1, 132.6, 134.7, 135.2, 139.1, 146.8, 168.0, 175.4, 180.9. HRMS-ESI m/z $[\text{M} + \text{H}]^+$ calcd for $\text{C}_{21}\text{H}_{16}\text{N}_3\text{O}_3$: 358.11862; found: 358.11862. $\Delta = 0$ ppm.

2.1.1.5. 2-(1-(4-methoxyphenyl)-1*H*-1,2,3-triazol-4-yl)-2,3-dihydronaphtho[2,3-*b*]furan-4,9-dione (**6c**). Yellow solid, m.p. 247-248 °C. IR (KBr, cm^{-1}): ν 1682, 1639, 1626, 1594, 1519, 1390, 1373, 1284, 1253, 1241, 1192, 1174, 1035, 958, 830, 722, 620. ^1H NMR (DMSO- d_6 , 500 MHz) δ ppm: 3.52 (dd, J 17.0 and 8.0 Hz, 1H), 3.64 (dd, J 17.0 and 10.5 Hz, 1H), 3.83 (s, 3H), 6.30 (dd, J 10.5 and 8.0 Hz, 1H), 7.14 (d, J 9.0 Hz, 2H), 7.80 (d, J 9.0 Hz, 2H), 7.82-7.88 (m, 2H), 7.99-8.02 (m, 2H), 8.98 (s, 1H). ^{13}C NMR (DMSO- d_6 , 125 MHz APT) δ ppm: 32.1, 55.5, 78.5, 114.8, 121.8, 122.5, 123.9, 125.4, 125.7, 130.0, 131.2, 132.2, 133.3, 134.3, 146.1, 158.7, 159.4, 177.0, 181.4. HRMS-ESI m/z $[\text{M} + \text{H}]^+$ calcd for $\text{C}_{21}\text{H}_{17}\text{N}_3\text{O}_4$: 374.111353; found: 374.111353. $\Delta = 0$ ppm.

2.1.1.6. 2-(1-(4-methoxyphenyl)-1H-1,2,3-triazol-4-yl)-2,3-dihydronaphtho[1,2-b]furan-4,5-dione (**7c**). Orange solid, m.p. 191-192 °C. IR (KBr, cm^{-1}): ν 1699, 1653, 1619, 1590, 1572, 1519, 1411, 1283, 1261, 1218, 1043, 992, 843, 827, 778. ^1H NMR (DMSO- d_6 , 500 MHz) δ ppm: 3.40 (dd, J 15.2 and 7.4 Hz, 1H), 3.53 (dd, J 15.2 and 10.5 Hz, 1H), 3.83 (s, 3H), 6.42 (dd, J 10.5 and 7.4 Hz, 1H), 7.14 (d, J 9.0 Hz, 1H), 7.64 (dd, J 7.5 and 1.5 Hz, 1H), 7.69 (td, J 7.8 and 1.3 Hz, 1H), 7.76 (td, J 7.8 and 1.3 Hz, 1H), 7.81 (d, J 9.0 Hz, 2H), (dd, J 7.5 and 1.5 Hz, 1H, 1H), 9.01 (s, 1H). ^{13}C NMR (DMSO- d_6 , 125 MHz APT) δ ppm: 31.5, 55.4, 80.0, 114.8, 114.9, 121.8, 122.3, 124.1, 126.8, 128.8, 129.7, 130.5, 131.6, 134.6, 146.0, 159.3, 167.4, 174.8, 180.3. HRMS-ESI m/z $[\text{M} + \text{H}]^+$ calcd for $\text{C}_{21}\text{H}_{17}\text{N}_3\text{O}_4$: 374.111353; found: 374.111353. $\Delta = 0$ ppm.

2.1.1.7. 2-(1-(4-nitrophenyl)-1H-1,2,3-triazol-4-yl)-2,3-dihydronaphtho[2,3-b]furan-4,9-dione (**6d**). Yellow solid, m.p. 246 °C. IR (KBr, cm^{-1}): ν 1681, 1625, 1594, 1531, 1504, 1459, 1343, 1244, 1190, 1254, 1020, 922, 955, 855, 833, 748, 720, 662. ^1H NMR (DMSO- d_6 , 500 MHz) δ ppm: 3.52 (dd, J 16.9 and 7.9 Hz, 1H), 3.68 (dd, J 16.9 and 7.9 Hz, 1H), 6.35 (dd, J 10.8 and 7.9 Hz, 1H), 7.81-7.89 (m, 2H), 7.99-8.03 (m, 2H), 8.23 (d, J 9.0 Hz), 8.46 (d, J 9.0 Hz), 9.30 (s, 1H). ^{13}C NMR (DMSO- d_6 , 125 MHz APT) δ ppm: 32.2, 78.2, 120.7, 122.9, 123.8, 125.3, 125.6, 131.2, 132.4, 133.2, 134.3, 140.6, 146.8, 147.0, 158.6, 176.9, 181.3. HRMS-ESI m/z $[\text{M} + \text{Na}]^+$ calcd for $\text{C}_{20}\text{H}_{13}\text{N}_4\text{NaO}_5$: 411.0699; found: 411.0700. $\Delta = 0.2$ ppm.

2.1.1.8. 2-(1-(4-nitrophenyl)-1H-1,2,3-triazol-4-yl)-2,3-dihydronaphtho[1,2-b]furan-4,5-dione (**7d**). Orange solid, m.p. 243-244 °C. IR (KBr, cm^{-1}): ν 1698, 1649, 1608, 1573, 1536, 1505, 1449, 1404, 1348, 1319, 1294, 1251, 1217, 1140, 1112, 1082, 1053, 1025, 889, 854, 832, 768, 747, 682, 657. ^1H NMR (DMSO- d_6 , 500 MHz) δ ppm: 3.40

(dd, *J* 15.5 and 7.5 Hz, 1H), 3.56 (dd, *J* 15.5 and 7.5 Hz, 1H), 6.48 (dd, *J* 10.5 and 7.5 Hz, 1H), 7.64 (dd, *J* 7.5 and 1.0 Hz 1H), 7.68-7.72 (m, 1H), 7.76-7.79 (m, 1H), 7.98 (dd, *J* 7.5 and 1.0 Hz, 1H), (8.24 (d, *J* 9.3 Hz), 8.46 (d, *J* 9.3 Hz), 9.33 (s, 1H). ¹³C NMR (DMSO-d₆, 125 MHz APT) δ ppm: 31.6, 79.6, 114.9, 120.7, 123.0, 124.2, 125.4, 126.8, 128.6, 130.5, 132.0, 134.7, 140.6, 146.8, 147.0, 167.4, 174.8, 180.3. HRMS-ESI *m/z* [M + H]⁺ calcd for C₂₀H₁₃N₄O₅: 389.08805; found: 389.08867. Δ = 0.2 ppm.

2.1.1.9. 2-(1-(4-fluorophenyl)-1H-1,2,3-triazol-4-yl)-2,3-dihydronaphtho[2,3-*b*]furan-4,9-dione (**6e**). Yellow solid, m.p. 248–249 °C. IR (KBr, cm⁻¹): ν 1681, 1624 (C-H Ar), 1582, 1513, 1454, 1371, 1328, 1283, 1237, 1190, 1098, 1054, 1022, 994, 955, 889, 831, 720, 653, 617. ¹H NMR (DMSO-d₆, 500 MHz) δ ppm: 3.52 (dd, *J* 17.0 and 7.9 Hz, 1H), 3.65 (dd, *J* 17.0 and 10.7 Hz, 1H), 6.32 (dd, *J* 10.7 and 7.9 Hz, 1H), 7.46 (t, *J* 8.8 Hz, 2H), 7.80-7.88 (m, 2H), 7.93-7.96 (m, 2H), 7.99-8.03 (m, 2H), 9.06 (s, 1H). ¹³C NMR (DMSO-d₆, 125 MHz APT) δ ppm: 32.7, 79.0, 117.2 (d, *J* 23.3 Hz), 123.1 (d, *J* 8.8 Hz), 123.4, 124.5, 125.0, 126.3, 131.8, 133.0, 133.5 (d, *J* 2.9 Hz), 133.9, 134.9, 147.0, 159.3, 162.3 (d, *J* 244.5 Hz), 177.6, 182.0. ¹⁹F RMN (DMSO-d₆, 470 MHz) δ ppm: -109.7 (bs, 1F). HRMS-ESI *m/z* [M + H]⁺ calcd for C₂₀H₁₃FN₃O₃: 362.09355; found: 362.09354. Δ = 0 ppm.

2.1.1.10. 2-(1-(4-fluorophenyl)-1H-1,2,3-triazol-4-yl)-2,3-dihydronaphtho[1,2-*b*]furan-4,5-dione (**7e**). Orange solid, m.p. 209-210 °C. IR (KBr, cm⁻¹): ν 1698, 1653 (C-H Ar), 1618, 1587, 1514, 1489, 1453, 1408, 1357, 1278, 1219, 1160, 1081, 1032, 993, 860, 833, 773, 720, 696, 657. ¹H NMR (DMSO-d₆, 500 MHz) δ ppm: 3.40 (dd, *J* 15.3 and 7.5 Hz, 1H), 3.54 (dd, *J* 15.3 and 10.3 Hz, 1H), 6.44 (dd, *J* 10.3 and 7.5 Hz, 1H), 7.46 (t, *J* 8.8 Hz, 2H), 7.64 (dd, *J* 7.5 and 0.5 Hz, 1H), 7.70 (td, *J* 7.5 and 1.1 Hz, 1H), 7.77 (td, *J* 8.3 and 1.1 Hz, 1H), 7.94-7.99 (m, 3H), 9.09 (s, 1H). ¹³C NMR (DMSO-d₆, 125

MHz APT) δ ppm: 32.1, 80.4, 115.5, 117.2 (d, J 23.3 Hz), 123.2 (d, J 8.8 Hz), 123.3, 124.8, 127.4, 129.2, 131.1, 132.6, 133.5 (d, J = 2.9 Hz), 135.2, 147.0, 162.3 (d, J 244.7 Hz), 168.0, 175.4, 180.9. ^{19}F RMN (DMSO- d_6 , 470 MHz) δ ppm: -109.7-109.7 (m, 1F). HRMS-ESI m/z $[\text{M} + \text{H}]^+$ calcd for $\text{C}_{20}\text{H}_{13}\text{FN}_3\text{O}_3$: 362.09355; found: 362.09354. Δ = 0 ppm.

2.1.1.11. 2-(1-(4-chlorophenyl)-1H-1,2,3-triazol-4-yl)-2,3-dihydronaphtho[2,3-*b*]furan-4,9-dione (**6f**). Yellow solid, m.p. 262-263 °C. IR (KBr, cm^{-1}): ν 1681, 1624 (C-H Ar), 1582, 1502, 1438, 1371, 1329, 1283, 1240, 1191, 1092, 1055, 1022, 955, 890, 857, 828, 721, 653. ^1H NMR (DMSO- d_6 , 500 MHz) δ ppm: 3.51 (dd, J 17.0 and 7.8 Hz, 1H), 3.65 (dd, J 17.0 and 11.0 Hz, 1H), 6.32 (dd, J 11.0 and 7.8 Hz, 1H), 7.68 (d, J 9.0 Hz, 2H), 7.81-7.89 (m, 2H), 7.95 (d, J 9.0 Hz, 2H), 7.99-8.03 (m, 2H), 9.13 (s, 1H). ^{13}C NMR (DMSO- d_6 , 125 MHz APT) δ ppm: 32.2, 78.4, 121.8, 122.6, 123.9, 125.4, 125.7, 129.8, 131.2, 132.4, 133.1, 133.3, 134.3, 135.2, 146.5, 158.7, 177.0, 181.4. HRMS-ESI m/z $[\text{M} + \text{H}]^+$ calcd for $\text{C}_{20}\text{H}_{13}\text{ClN}_3\text{O}_3$: 378.06400; found: 378.06399. Δ = 0 ppm.

2.1.1.12. 2-(1-(4-chlorophenyl)-1H-1,2,3-triazol-4-yl)-2,3-dihydronaphtho[1,2-*b*]furan-4,5-dione (**7f**). Orange solid. m.p. 236-237 °C. IR (KBr, cm^{-1}): ν 1694, 1655, 1620, 1574, 1502, 1453, 1408, 1357, 1274, 1249, 1218 1142, 1080, 990, 868, 826, 777, 756, 698, 657. ^1H NMR (DMSO- d_6 , 500 MHz) δ ppm: 3.40 (dd, J 15.4 and 7.4 Hz, 1H), 3.54 (dd, J 15.4 and 10.3 Hz, 1H), 6.44 (dd, J 10.3 and 7.4 Hz, 1H), 7.63-7.71 (m, 3H), 7.75-7.78 (m, 1H), 7.93-7.99 (m, 3H), 9.14 (s, 1H). ^{13}C NMR (DMSO- d_6 , 125 MHz APT) δ ppm: 31.5, 79.8, 114.9, 121.8, 122.6, 124.1, 126.8, 128.6, 129.7, 130.5, 132.0, 133.1, 134.7, 135.2, 146.5, 167.4, 174.8, 180.3. HRMS-ESI m/z $[\text{M} + \text{H}]^+$ calcd for $\text{C}_{20}\text{H}_{13}\text{ClN}_3\text{O}_3$: 378.06400; found: 378.06399. Δ = 0 ppm.

2.1.1.13. 2-(1-(3,4-dichlorophenyl)-1H-1,2,3-triazol-4-yl)-2,3-dihydronaphtho[2,3-*b*]furan-4,9-dione (**6g**). Yellow solid, m.p. 225-226 °C. IR (KBr, cm^{-1}): ν 1680, 1624, 1581, 1487, 1437, 1370, 1282, 1240, 1190, 1132, 1053, 1026, 956, 881, 856, 812, 750, 721, 679. ^1H NMR (DMSO- d_6 , 500 MHz) δ ppm: 3.49 (dd, J 16.9 and 7.9 Hz, 1H), 3.67 (dd, J 16.9 and 10.8 Hz, 1H), 6.33 (dd, J 10.8 and 7.9 Hz, 1H), 7.81-7.89 (m, 3H), 7.95-8.03 (m, 3H), 8.25 (d, J 3.0 Hz, 1H), 9.18 (s, 1H). ^{13}C NMR (DMSO- d_6 , 125 MHz APT) δ ppm: 32.2, 78.2, 120.1, 121.9, 122.8, 123.8, 125.4, 125.7, 131.2, 131.7, 132.2, 132.4, 133.3, 134.4, 133.3, 135.9, 146.7, 158.6, 177.0, 181.4. HRMS-ESI m/z [$\text{M} + \text{H}$] $^+$ calcd for $\text{C}_{20}\text{H}_{12}\text{Cl}_2\text{N}_3\text{O}_3$: 412.02502; found: 412.02502. $\Delta = 0$ ppm.

2.1.1.14. 2-(1-(3,4-dichlorophenyl)-1H-1,2,3-triazol-4-yl)-2,3-dihydronaphtho[1,2-*b*]furan-4,5-dione (**7g**). Orange solid, m.p. 242-243 °C. IR (KBr, cm^{-1}): ν 1697, 1651 (C-H Ar), 1614, 1572, 1487, 1438, 1410, 1362, 1279, 1251, 1219, 1166, 1133, 1083, 1030, 1005, 868, 813, 770, 719, 677, 625. ^1H NMR (DMSO- d_6 , 500 MHz) δ ppm: 3.38 (dd, J 15.4 and 7.2 Hz, 1H), 3.55 (dd, J 15.4 and 10.4 Hz, 1H), 6.45 (dd, J 10.4 and 7.2 Hz, 1H), 7.64 (d, J 8.0 Hz, 1H), 7.67-7.79 (m, 3H), 7.89 (d, J 8.5 Hz, 3H), 7.96-7.99 (m, 2H), 8.26 (d, J 2.5 Hz, 1H), 9.21 (s, 1H). ^{13}C NMR (DMSO- d_6 , 125 MHz APT) δ ppm: 31.6, 79.7, 114.9, 120.2, 121.9, 122.8, 124.2, 126.8, 128.6, 130.5, 131.2, 131.7, 132.0, 132.3, 134.7, 135.9, 146.7, 167.4, 174.8, 180.3. HRMS-ESI m/z [$\text{M} + \text{H}$] $^+$ calcd for $\text{C}_{20}\text{H}_{12}\text{Cl}_2\text{N}_3\text{O}_3$: 412.02502; found: 412.02502. $\Delta = 0$ ppm.

2.1.1.15. 2-(1-(2,5-dichlorophenyl)-1H-1,2,3-triazol-4-yl)-2,3-dihydronaphtho[2,3-*b*]furan-4,9-dione (**6h**). Yellow solid, m.p. 214-215 °C. IR (KBr, cm^{-1}): ν 1672, 1624, 1591, 1491, 1487, 1491, 1487, 1451, 1371, 1332, 1292, 1236, 1191, 1097, 1050, 946, 825, 718, 688. ^1H NMR (DMSO- d_6 , 500 MHz) δ ppm: 3.53 (dd, J 16.8 and 8.3 Hz, 1H), 3.66 (dd, J 16.8 and 10.5 Hz, 1H), 6.35 (dd, J 10.5 and 8.3 Hz, 1H), 7.74 (dd, J 8.3 and

2.5 Hz, 1H), 7.81-7.84 (m, 2H), 7.85-7.88 (m, 1H), 7.94 (d, J 2.5 Hz, 1H), 7.99-8.02 (m, 2H), 8.89 (s, 1H). ^{13}C NMR (DMSO- d_6 , 125 MHz APT) δ ppm: 31.1, 78.2, 123.9, 125.4, 125.7, 126.5, 127.4, 128.1, 131.2, 131.5, 131.9, 132.4, 132.4, 133.3, 134.3, 135.1, 145.3, 158.7, 177.0, 181.4. HRMS-ESI m/z $[\text{M} + \text{H}]^+$ calcd for $\text{C}_{20}\text{H}_{12}\text{Cl}_2\text{N}_3\text{O}_3$: 412.02502; found: 412.02502. $\Delta = 0$ ppm.

2.1.1.16. *2-(1-(2,5-dichlorophenyl)-1H-1,2,3-triazol-4-yl)-2,3-dihydronaphtho[1,2-b]furan-4,5-dione (7h)*. Orange solid, m.p. 207-208 °C. IR (KBr, cm^{-1}): ν 1697, 1657, 1624, 1588, 1486, 1448, 1407, 1354, 1277, 1235, 1211, 1140, 1101, 1081, 1030, 1010, 860, 826, 772, 720, 698, 657, 631. ^1H NMR (DMSO- d_6 , 500 MHz) δ ppm: 3.40 (dd, J 15.2 and 7.5 Hz, 1H), 3.55 (dd, J 15.2 and 10.4 Hz, 1H), 6.47 (dd, J 10.4 and 7.5 Hz, 1H), 7.64 (dd, J 7.5 and 1.0 Hz, 1H), 7.68-7.79 (m, 4H), 7.82 (d, J 9.0 Hz, 1H), 7.95 (d, J 2.5 Hz, 1H), 7.98 (dd, J 7.8 and 0.8 Hz, 1H), 8.91 (s, 1H). ^{13}C NMR (DMSO- d_6 , 125 MHz APT) δ ppm: 31.6, 79.6, 114.9, 124.2, 126.4, 126.8, 127.4, 128.1, 128.6, 130.5, 131.5, 131.8, 132.0, 132.4, 134.6, 135.1, 145.4, 167.4, 174.8, 180.2. HRMS-ESI m/z $[\text{M} + \text{H}]^+$ calcd for $\text{C}_{20}\text{H}_{12}\text{Cl}_2\text{N}_3\text{O}_3$: 412.02502; found: 412.02502. $\Delta = 0$ ppm.

2.2. Biological Assays

2.2.1. Materials

The Caco-2, Calu-3, MDA-MB231 and Vero cell lines were purchased from the Rio de Janeiro Cell Bank, Brazil. Dulbecco's Modified Eagles Medium (DMEM), Ross Park Memorial Institute Medium (RPMI-1640), Hank's Balanced Salt Solution (HBSS), foetal bovine serum (FBS), antibiotic solution (10,000 U/mL penicillin and 10mg/mL streptomycin), antifungal solution (25-30 $\mu\text{g}/\text{mL}$ amphotericin B), trypsin-EDTA

solution (2.5 mg/mL trypsin, 0.2mg/mL EDTA) and 3-(4,5-dimethylthiazol-2-yl)-2,5-diphenyltetrazolium bromide (MTT) were all supplied by Sigma–Aldrich (São Paulo, Brazil). Dimethyl sulfoxide (DMSO) and other reagents were from analytical grade.

2.2.2. Cell line culture conditions

The Caco-2 (colon adenocarcinoma), Calu-3 (lung adenocarcinoma), MDA-MB231 (mammary gland adenocarcinoma) and Vero cell lines were maintained in DMEM supplemented with 4.5 mg/ml glucose, 0.1 mg/ml penicillin, 0.14 mg/ml streptomycin and 10 % inactivated FBS. Cultured cells were maintained at 37 °C in an atmosphere containing 95% air and 5 % CO₂. Cells were sub-cultivated every 48h by trypsin–EDTA solution.

2.2.3. Cytotoxicity by MTT assay

Metabolically active cells were assessed using the MTT reduction colorimetric assay, as reported by Mosmann [16] and Alley [17]. Cells were seeded in 96-well plates (Corning) at density of 32,000 cells/well, distributed in a total volume of 200 µL/well. Plates were taken to cell incubator at 37 °C and 5 % CO₂ for 24 hours. After incubation, cells were placed in contact with the samples (5 to 400 µM) for 48 hours. Samples were solubilized in 10 % FBS DMEM or RPMI containing 0.5 % of DMSO. The control group was represented by the mixture between the culture media and DMSO (0.5 %). The samples were aspirated and treated with MTT reagent by adding 100 µL of HBSS and 25µL of MTT solution (2.5 mg/mL) per well. The plates containing the cells were incubated with MTT for 3 hours at 37 °C and 5 % CO₂. At the end of incubation time, MTT was aspirated and the cells were washed with phosphate buffer solution (PBS)

(pH 7.4). The phosphate buffer was then aspirated and 100 μ L/well of DMSO were added to break cell membrane and solubilize formazan crystals. The absorbance readings were performed in Microplate Absorbance Reader iMARK™ (Bio-Rad Laboratories Srl, Segrate, Italy), with reference to 570 nm and 690 nm after vigorous shaking during 60 seconds [16, 17].

Cytotoxicity was expressed as the percentage of cells surviving after treatment with samples in comparison to untreated cells. Drug concentration required to inhibit cell growth by 50 % (IC_{50} for tumor cells and CC_{50} for Vero cells) and selectivity index (SI) were calculated with GraphPad Prism 5 (version 5.00; GraphPad Software, Inc., San Diego, CA, USA). In some circumstances, the samples that presented statistically significant differences from control group were not selected for IC_{50} assays due to the lack of biological relevance of the data, i.e., statistical significance without adequate level of cell viability. Thus, IC_{50} studies were carried out only with substances with high toxicity (cell viability decreased by 50 %) on at least one tumor cell line and simultaneously cell viability percentage above 70 % in Vero cells, which meets the criteria defined by ISO 10993:5 [18].

2.2.4. *In vitro* hemocompatibility studies

All human blood samples were obtained from adult volunteers, healthy, 18-35 years, not using drugs or other substances that could interfere with the experiment, for at least 15 days (Ethics Committee – ID number: 2.364.834).

The hemocompatibility evaluation of the best dihydronaphthoquinone derivative with antitumor activity was performed through the hemolysis, platelet aggregation, prothrombin time (PT) and activated partial thromboplastin time (aPTT) assays. All samples were used at 100 μ M and the vehicle (DMSO) did not exceeded 1 % in the

tests. In hemolysis test, healthy erythrocytes were washed 3 times with PBS (pH 7.4) by centrifugation. Then, the derivative was incubated with the erythrocytes suspension for 3 h at 37 °C. The release of hemoglobin was determined by the optical density of the supernatant at 540 nm. The experiment was performed in triplicate and the complete hemolysis (positive control) was determined by using 1 % Triton X-100 (Sigma Aldrich, USA) [19-21]. The platelet aggregation assay was performed by turbidimetric method using Chronolog[®] Model 560 lumi-aggregometer (Chrono-Log Corporation, Havertown, PA). In this evaluation, the derivative (100 µM) was pre-incubated for 2 minutes at 37 °C in fresh PRP (platelet-rich plasma) before the addition of the platelet agonist. Maximal aggregation was obtained by stimulating platelets with arachidonic acid (500 mM) (Cayman Chemical Co., Inc., Ann Arbor, MI). The inhibition of platelet aggregation was obtained using acetylsalicylic acid (100 µM) (Sigma Aldrich, USA) as positive control [22,23]. The PT and aPTT assays were performed by using citrated platelet poor plasma (PPP). Assays were performed in coagulation analyzer CoagLab[®] IV (Beijing Shining Sun Technology Co., Ltd., China) and anticoagulant profile (positive control) was obtained using rivaroxaban (100 µM) (BioChemPartner, Wuhan, China) [23,24]. Negative control, for all hemocompatibility tests, was DMSO 1%.

2.2.5. Molecular modeling studies

The molecular structure of **7a**, (the most promising compound according to the biological assays) was constructed in neutral state using Spartan'10 program (Wavefunction Inc. Irvine, CA, USA). The neutral state of this compound was selected for this study accordingly to the protonation state at pH 7.4 predicted by MarvinSketch v. 16.2.29.0, 2016, ChemAxon (<http://www.chemaxon.com>). This structure was submitted to a conformational analysis using the Merck Molecular Force Field

(MMFF). Then, the lowest energy conformer was selected for further geometry optimization in vacuum using the RM1 semi-empirical method. Finally, the structure was submitted to a single point *ab initio* calculation using the Hartree-Fock method with 6-31G* basis set. The final optimized structure with electrostatic charges was used for docking studies.

Meanwhile, the structures of the potential biological targets were obtained from Protein Data Bank with the following codes: human topoisomerase I (1K4T), topoisomerase II α including ATPase domain (1ZXM) and DNA-binding domain (5GWK) and topoisomerase II β (3QX3) [25-27]. Solvent molecules and ligands were removed from protein structures.

Molecular docking studies were performed using Autodock Vina 1.1.2 [28]. Initially, the protein structures were prepared using Autodock Tools 1.5.7 by adding polar hydrogen and assigning Gasteiger charges and all rotatable bonds of the ligand were allowed to rotate freely during docking studies. The cubic grid box was centered on the ligand and presented the dimensions of 20 Å³ for topoisomerase I, 18 Å³ for topoisomerase II α ATPase domain, 26 Å³ for topoisomerase II α DNA-binding domain and 20 Å³ for topoisomerase II β . The default search parameters values were used. The lowest binding energy pose obtained in the docking of **7a** with each enzyme was selected and interactions analysis were carried out using Pymol v. 1.2r2 (The PyMOL Molecular Graphics System, Version 1.2r2 Schrödinger, LLC).

2.2.6. Statistical Analysis

All experimental results (average and standard deviation) were statistically evaluated in Sigma Plot 12.5 software. The t-test was used for comparative evaluations of these results where a p-value ≤ 0.05 was considered statistically significant.

3. Results and Discussion

3.1. Chemistry

Initially, the 4-vinyl-1*H*-1,2,3-triazoles **4a-h** were prepared according to the reported methodology [29,30] from the protocol based on a Huisgen 1,3-dipolar cycloaddition. The reaction between several aryl azides (from anilines **3a-h**) and a propargylic alcohol was catalyzed by Cu(I), providing only the 1,4-disubstituted regioisomer, followed by partial oxidation of the alcohol to generate the 4-carboxaldehyde-1*H*-1,2,3-triazoles. The Wittig reaction allowed to prepare the 4-vinyl-1*H*-1,2,3-triazoles (**4a-h**) with overall yields ranging from 80-99 % (Fig. 2). All obtained derivatives presented spectroscopic data in agreement with described report.

The reaction proposed to synthesize the hybrids naphthoquinone-1,2,3-triazoles was a radical electrocyclic reaction between 2-hydroxy-1,4-naphthoquinone **5** and the 4-vinyl-1*H*-1,2,3-triazoles (**4a-h**) that have been reported in the literature by several authors (Fig. 2) [30]. Thus, the reactions were carried out in presence of an excess cerium (IV) ammonium nitrate as one-electron oxidizing agent, in dried acetonitrile, at low temperature and monitored by thin layer chromatography (TLC). After 3 hours of reaction time it was observed total consumption of **5** a remaining small amounts of unreacted **4** and the formation of two more polar products (a yellow spot and an orange more polar spot). After the evaporation of the solvent and purification of the reaction mixture by column chromatography using chloroform/ethyl acetate gradient as eluent, followed by spectroscopic analysis of each synthesized compound, it was possible to identify the compounds **6a-h** (yellow solid compounds) and **7a-h** (orange solid compounds). Considering the conversions of **5** in these isolated two isomers the yields

ranged from 40 to 59 %. In the Table 1 are described the ratio between **6:7** and the overall.

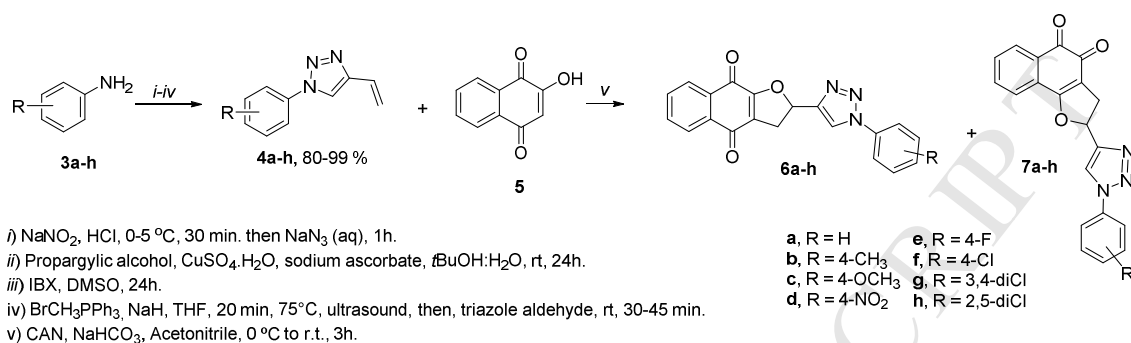


Fig. 2. Synthesis of isomeric hybrids **6a-h** and **7a-h**

Table 1. Chemical conversion of compounds **6** and **7**

Entry	Compounds	R	Ratio (6 : 7)	Conversion (%)
1	6a	H	1 : 1.3	55
2	7a			
3	6b	4- CH_3	1 : 1.7	59
4	7b			
5	6c	4- OCH_3	1 : 1.7	47
6	7c			
7	6d	4- NO_2	1 : 1.3	55
8	7d			
9	6e	4-F	1 : 1.4	40
10	7e			
11	6f	4-Cl	1 : 1.4	59
12	7f			
13	6g	3,4-diCl	1 : 1.4	56
14	7g			
15	6h	2,5-diCl	1 : 1.5	58
16	7h			

The structures of the compounds were elucidated by spectroscopic techniques (see Experimental Section and Supplementary Information). The ^1H NMR spectrum analysis of compound **6b**, it could be observed two double doublets at 3.52 ppm (dd, J 17.0 and 7.9 Hz, 1H) and 3.65 ppm (dd, J 17.0 and 10.9 Hz, 1H) corresponding to H-3 protons; it was also observed a double doublet at 6.31 ppm (dd, J 10.9 and 7.9 Hz, 1H) corresponding to H-2 proton (see Fig. 2 for numbering) and the typical benzoaromatic pattern of 1,4-naphthoquinone isomers as multiplets at 7.80-7.88 ppm (m, 2H) and 7.99-8.03 ppm (m, 2H). The ^1H NMR spectrum of **7b**, it can be observed two double doublets at 3.40 ppm (dd, J 15.3 and 7.5 Hz, 1H) and 3.53 ppm (dd, J = 10.5 and 15.3 Hz, 1H) corresponding to H-3 protons; it was also observed a double doublet at 6.43 ppm (dd, J 10.5 and 7.5 Hz, 1H) corresponding to H-2 proton and the typical benzoaromatic pattern of 1,2-naphthoquinone isomers as one multiplet at 7.62-7.74 ppm corresponding to three protons (H-7, H-8 and H-9) and at a lower field one double doublet at 7.97 ppm (dd, J 8.0 and 1.0 Hz, 1H) referring to H-6 proton. Moreover, in the aromatic region, the singlet at 9.03 ppm assigned to the resonance of the H-5' proton for isomer **6b** and at 9.07 ppm for **7b**, a very characteristic signal of the proton resonance of triazolic ring CH.

3.2. Biological Assays

3.2.1. *In vitro* evaluation of the anticancer and toxicological profile

The hybrids naphthoquinone-1,2,3-triazoles **6a-h** and **7a-h** were screened *in vitro* activity against MDA-MB231, Caco-2 and Calu-3 human cancer cell lines and by

the absence of toxic effects (cell viability $\geq 70\%$) on Vero cells, using MTT reduction assay. The results are expressed in Table 2.

Table 2. Cell viability of cancer cell lines (Caco-2, Calu-3 and MDA-MB231) and Vero cells after 48 hours of exposition to hybrids naphthoquinone-1,2,3-triazoles **6a-h** and **7a-h** at 5 μM . Data are presented as mean \pm standard deviation

Compounds (5 μM)	Cell lines			
	Vero	Caco-2	Calu-3	MDA-MB231
6a	76.21 \pm 14.33	88.29 \pm 15.44	113.49 \pm 9.48	108.73 \pm 2.01
7a	67.97 \pm 10.20	23.92 \pm 0.58	110.34 \pm 17.78	87.72 \pm 3.44
6b	74.03 \pm 6.37	88.03 \pm 3.63	111.60 \pm 19.72	95.33 \pm 2.41
7b	41.80 \pm 5.48	33.27 \pm 2.84	110.88 \pm 14.63	90.71 \pm 3.37
6c	64.79 \pm 7.54	81.81 \pm 2.11	125.48 \pm 2.82	99.56 \pm 5.69
7c	34.14 \pm 1.10	23.04 \pm 3.43	112.65 \pm 5.16	41.10 \pm 5.59
6d	63.64 \pm 3.78	95.49 \pm 10.18	119.97 \pm 2.33	97.44 \pm 2.46
7d	88.65 \pm 25.20	86.89 \pm 4.26	132.93 \pm 6.43	99.24 \pm 4.35
6e	72.98 \pm 8.08	77.32 \pm 5.79	104.43 \pm 4.92	97.90 \pm 4.45
7e	55.84 \pm 1.85	37.89 \pm 8.28	117.46 \pm 8.99	41.49 \pm 2.97
6f	78.11 \pm 16.08	82.12 \pm 7.68	134.31 \pm 7.88	103.37 \pm 3.89
7f	59.29 \pm 9.67	46.42 \pm 17.74	122.25 \pm 8.43	46.55 \pm 5.82
6g	78.67 \pm 9.35	83.94 \pm 5.66	110.98 \pm 11.39	96.62 \pm 4.49
7g	80.99 \pm 8.41	94.38 \pm 4.52	110.70 \pm 8.94	90.22 \pm 1.13
6h	90.37 \pm 14.71	85.75 \pm 4.17	139.05 \pm 4.92	103.83 \pm 5.69
7h	74.70 \pm 4.41	78.12 \pm 4.95	117.82 \pm 7.99	82.09 \pm 6.29

Significance levels for statistical tests (t-test) are marked with * when p-value ≤ 0.001 and ** when $0.001 < \text{p-value} \leq 0.05$. The groups with no statistically significant differences were not marked (p-value > 0.05).

In vitro screening clearly demonstrated that only lung adenocarcinoma cells (Calu-3) were not affected by derivatives in MTT assay, since cell viability values

exceeded 100 %, i.e., cells were stimulated by the hybrids naphthoquinone-1,2,3-triazoles **6a-h** and **7a-h**. The compounds **7a-h** were selectively cytotoxic activity against colon and / or mammary gland adenocarcinoma cells.

MDA-MB231 cells were sensitized by **7c**, **7e** and **7f** (cell viability lower than 50 % - p -value ≤ 0.05), however these compounds were also toxic to Vero cells, and for this reason, determination of selectivity index between Vero and MDA-MB231 cells would not be relevant in this study.

Caco-2 cells have their viabilities decreased when exposed to derivatives **7a**, **7b**, **7c**, **7e**, **7f** (p -value ≤ 0.05). However, these derivatives also decreased Vero cells viability (< 70 %), with exception of **7a** (67.97 ± 10.20), which was evaluated by IC_{50} in Caco-2 cells ($4.48 \pm 0.71 \mu\text{M}$) and CC_{50} in Vero cells ($28.00 \pm 7.88 \mu\text{M}$). Finally, we found that **7a** was six times more selective for Caco-2 than Vero cells ($SI = 6.25$), indicating the potential of this compound as future drug candidate.

Through the hemocompatibility studies it was possible to observe that **7a** does not affect the platelet aggregation induced by arachidonic acid, in addition, this derivative did not interfere in prothrombin time (PT) and activated thromboplastin time (APTT), preserving integrates the activation of blood coagulation by extrinsic and intrinsic pathway. Interesting, **7a** showed no significant hemolytic profile after 3 hours incubation reinforcing their good safety degree (Fig. 3).

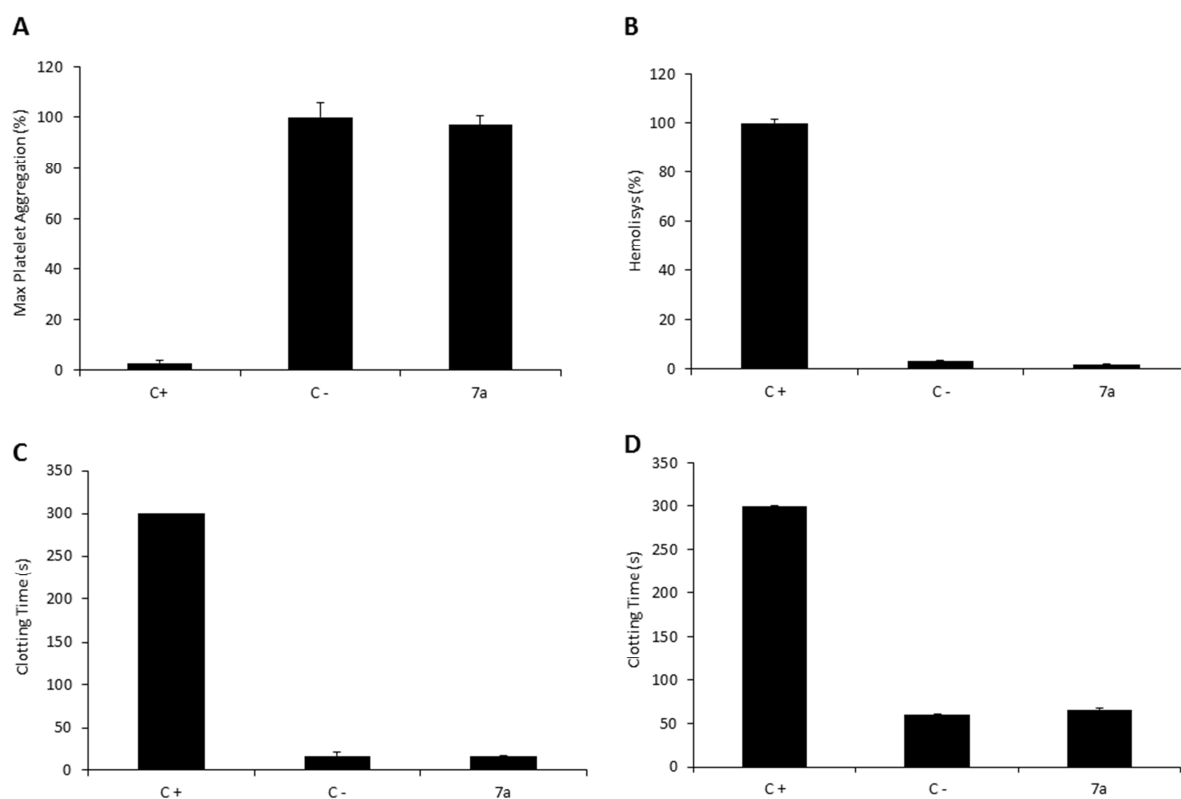


Fig. 3. Hemocompatibility Evaluation. (A) Platelet Aggregation Assay: (C-) DMSO 1 % and (C+) ASA 100 μ M. (B) Hemolysis Assay: (C-) DMSO 1 % and (C+) Triton x-100 1%. (C) Prothrombin Time (PT) Test: (C-) DMSO 1 % and (C+) Rivaroxaban 100 μ M. (D) Activated partial thromboplastin time (APTT) Test: (C-) DMSO 1 % and (C+) Rivaroxaban 100 μ M **7a** (100 μ M).

3.2.2 Molecular docking studies

The naphthoquinones are widely explored as potential anticancer agents and one of their mechanisms of action described is the apoptosis induction through topoisomerase enzymes inhibition [31-33]. Additionally, the dihydronaphthoquinone moiety can mimic the polycyclic nucleus of known topoisomerase inhibitors (Fig. 4). Thereby, in order to investigate the possible mechanism of action of **7a**, we carried out

docking studies with topoisomerase enzymes and compared with the crystal structure of topoisomerases with known inhibitors.

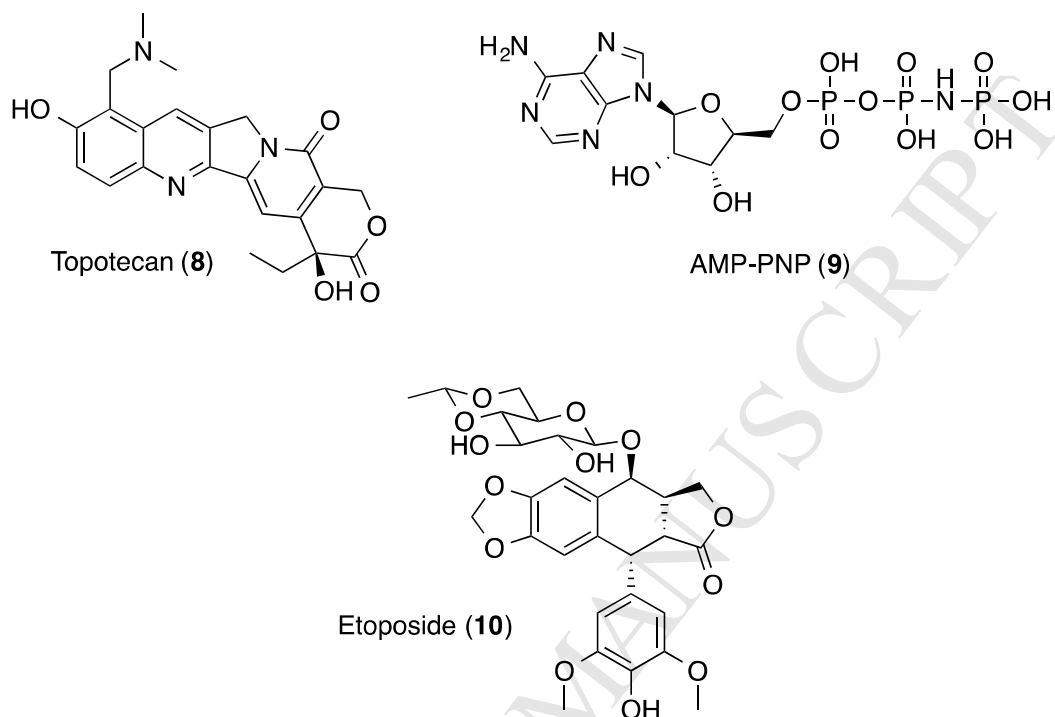


Fig. 4. 2D structures of the co-crystallized inhibitor of topoisomerase I (topotecan) and of topoisomerase II (etoposide and AMP-PNP).

First, we validated our docking protocol by redocking the co-crystallized inhibitors topotecan (8) in topoisomerase I, etoposide (10) in topoisomerase II α and II β and adenylyl-imidodiphosphate (AMP-PNP) (9) in ATPase domain of topoisomerase II α . All the ligands in the docking complexes conserved the same binding mode and interactions in the docking complexes in comparison to the crystal structures, which were evidenced by the root mean square deviation (RMSD) values obtained: topotecan (0.77 Å), AMP-PNP (0.49 Å), etoposide in topoisomerase II α (0.63 Å) and etoposide in topoisomerase II β (0.34 Å). According to the literature, successful docking prediction is achieved when RMSD is lower than 2.0 [34-36].

Thus, we applied these protocols for docking studies of **7a**. Since this compound has one chiral center, we docked both enantiomers, (*R*)-**7a** and (*S*)-**7a**, into the enzymes active site. Both compounds bound between the base pairs +1G/+1C and -1T/-1A, but they exhibited different binding modes. The results suggested that the *S*-enantiomer may be the most efficient enantiomer and main responsible for the activity as it presented the most similar binding mode in comparison to the known ligands, then, we focused our discussion on this enantiomer binding mode with topoisomerase enzymes (Fig. 5).

Docking of **7a** in topoisomerase I showed that this compound bound between the base pairs +1G/+1C and -1T/-1A (Fig. 5). The dihydronaphthoquinone moiety of this compound was π -stacked with +1G, -1T and -1A as observed for the drug topotecan (**8**). In addition, this nucleus was involved in hydrogen bonds with +1G and R364 which are important interactions described in the literature for other topoisomerase I inhibitors [37]. Meanwhile, the triazole and phenyl rings were positioned towards DNA major groove, allowing van der Waals contacts with M428 which may also contribute to the complex stabilization. The similar binding mode of **7a** with topotecan resulted in a great theoretical affinity to topoisomerase I, with a binding energy value of -11.5 Kcal/mol.

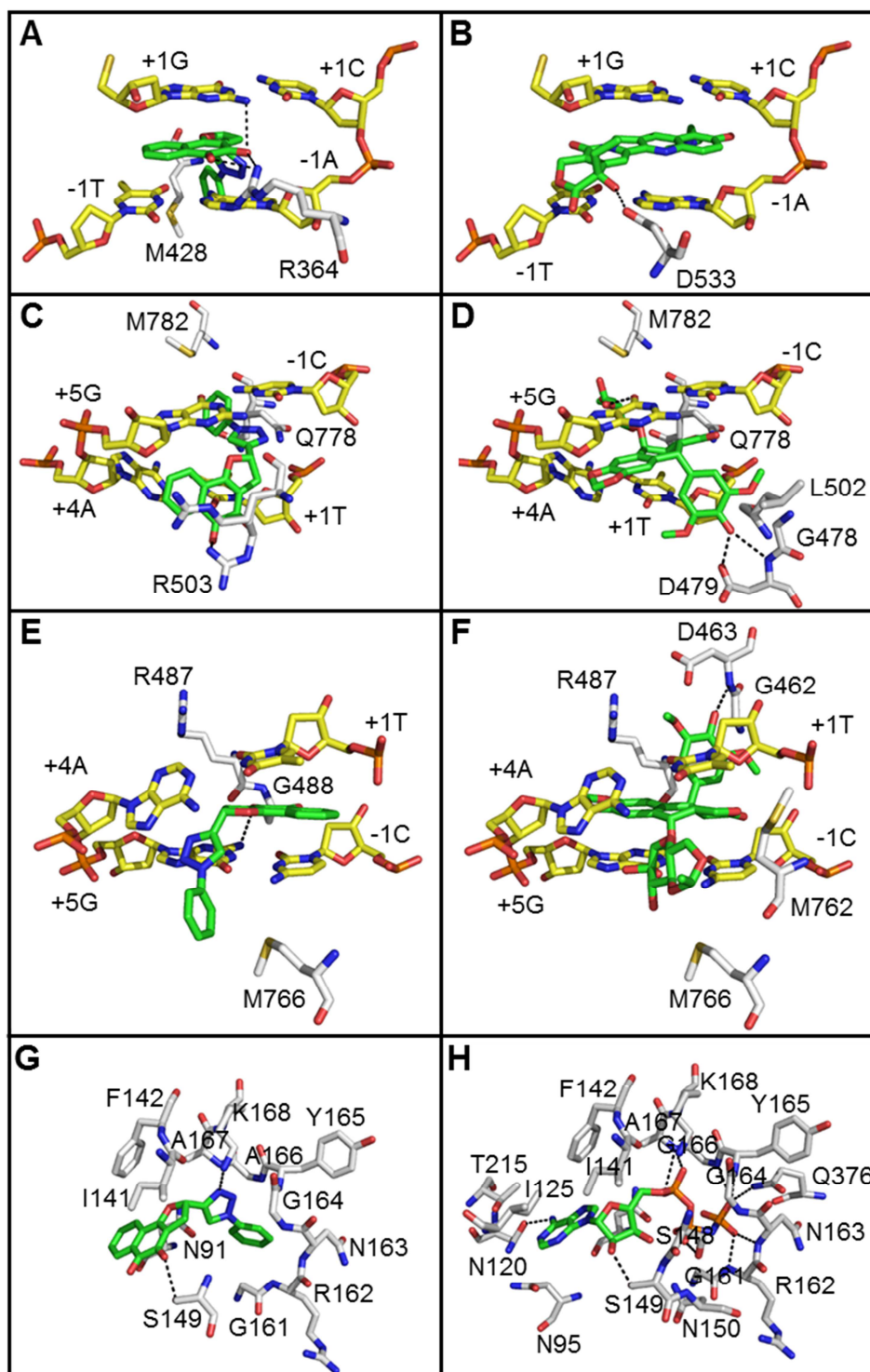


Fig. 5. Binding mode of **7a** in topoisomerases I and II in comparison to known inhibitors of these enzymes. In the first line are the complexes of topoisomerase I with (A) *(S)*-**7a** and (B) topotecan (**8**); in the second line are the complexes of topoisomerase II β with (C) *(S)*-**7a** and (D) etoposide (**10**); in the third line are the complexes of the DNA-binding domain of topoisomerase II α with (E) *(S)*-**7a**, and (F); in the fourth line

are the complexes of the ATPase domain of topoisomerase II α with (G) (S)-**7a**, and (H) AMP-PNP (**9**). Carbon atoms of the ligands were depicted in green, nucleotides in yellow and amino acid residues in white. Ionic interactions and hydrogen bonds are represented as dashed lines.

Moreover, we performed the docking studies of **7a** in topoisomerase II β which showed that this compound intercalated between base pairs +1T/+4A and -1C/+5G similar to etoposide (Fig. 5). We observed that the triazole ring of **7a** was π -stacked with -1C and +1T while phenyl group and tricyclic nucleus protruded towards DNA major and minor grooves, respectively, allowing van der Waals contacts with Q778 and M782 and also a hydrogen bond interaction with R503. **7a** conserved contacts observed for etoposide and other topoisomerase II β inhibitors (*e.g.* R503, M782 and Q778) [38]. However, the dihydronaphthoquinone moiety of this compound was not stacked with the nitrogenous-containing bases as expected for naphthoquinones with topoisomerase II β inhibitory activity.

Further, we investigated whether this compound may act on topoisomerase II α (Fig. 5). As observed for etoposide, the compound bound between the base pairs +5G/-1C and +4A/+1T with low binding energy (-10.1 Kcal/mol). The dihydronaphthoquinone moiety was positioned similar to the polycyclic nucleus of the etoposide and π -stacked with +1T and -1C nucleobases while hydrogen bond interaction was observed with +5G. R487 and G488 were also involved in van der Waals contacts with this nucleus. Interestingly, the triazole and phenyl rings of this compound was positioned towards DNA major groove as observed for the glycoside moiety of etoposide, conserving van der Waals contact with M766.

As the inhibition of the ATPase function of topoisomerase II α is also a possible mechanism of action for the cytotoxic activity of naphthoquinone derivatives [39], we

docked **7a** in the ATP binding site of this enzyme (Fig. 5). It exhibited a similar binding mode than the known inhibitor with low binding energy (-11.2 Kcal/mol). The dihydronaphthoquinone nucleus bound in the same site of adenine and ribose groups of AMP-PNP, exploring van der Waals contacts with N91, I141 and F142 and, additionally, the hydrogen bond interaction with S149 was conserved. The triazole and phenyl groups were positioned in the phosphate binding site region, making contacts with G161, R162, N163, G164, Y165, G166, A167 and K168 like AMP-PNP [26].

4. Conclusions

A series of hybrids naphthoquinone-1,2,3-triazoles have been evaluated for in vitro cytotoxic activity against human tumor cell lines (MDA-MB231, Calu-3 and Caco-2) and healthy cells (Vero). Compound **7a** exhibited the most promising profile due to its selective cytotoxic action against colon adenocarcinoma cells. Based on docking studies, we suggest that **7a** may inhibit topoisomerase I and II α due to the similarities in the binding mode and interactions in comparison to known inhibitors but not topoisomerase II β and the blockage of topoisomerase I and II α may be one of the mechanisms of action responsible for the cytotoxic effect of **7a** in Caco-2 cells. These results encourage new studies of molecular mechanism and the development of more potent and selective derivatives.

Supporting information

Supporting information includes physical and spectroscopic information for compounds

Acknowledgments

The authors would like to thank to National Council of Research of Brazil (CNPq), Coordination for the Improvement of Higher Education Personnel (CAPES) and Carlos Chagas Filho Research Support Foundation of the state of Rio de Janeiro (FAPERJ) for funding this work and for Research and Post-graduation fellowships.

Conflict of Interest

The authors declare that there are no conflicts of interest.

References

- [1] F.C. da Silva, V.F. Ferreira, Natural Naphthoquinones with Great Importance in Medicinal Chemistry, *Curr. Org. Synth.* 13 (2016) 334-371.
- [2] C.A. Camara, T.M. Silva, T.G. da-Silva, R.M. Martins, T.P. Barbosa, A.C. Pinto, M.D. Vargas, Molluscicidal activity of 2-hydroxy-[1,4]naphthoquinone and derivatives, *An. Acad. Bras. Ciênc.* 80 (2008) 329-334.
- [3] T.P. Barbosa, C.A. Câmara, T.M.S. Silva, R.M. Martins, A.C. Pinto, M.D. Vargas, New 1,2,3,4-tetrahydro-1-aza-anthraquinones and 2-aminoalkyl compounds from norlapachol with molluscicidal activity, *Bioorg. Med. Chem.* 13 (2005) 6464-6469.
- [4] V.F. Ferreira, A. Jorqueira, A.M.T. Souza, M.N. da Silva, M.C.B.V. de Souza, R.M. Gouvea, C.R. Rodrigues, A.V. Pinto, H.C. Castro, D.O. Santos, H.P. Araújo, S.C. Bourguignon, Trypanocidal agents with low cytotoxicity to mammalian cell line: A comparison of the theoretical and biological features of lapachone derivatives, *Bioorg. Med. Chem.* 14 (2006) 5459-5466.

- [5] A. Jorqueira, R.M. Gouvêa, V.F. Ferreira, M.N. da Silva, M.C.B.V. de Souza, A.A. Zuma, D.F.B. Cavalcanti, H.P. Araújo, S.C. Bourguignon, Oxirane derivative of α -lapachone is potent growth inhibitor of *Trypanosoma cruzi* epimastigote forms, *Parasitol. Res.* 99 (2006) 429-433.
- [6] E.N. Silva-Jr, R.F.S. Menna-Barreto, M.C.F.R. Pinto, R.S.F. Silva, D.V. Teixeira, M.C.B.V. de Souza, C.A. Simone, S.L. de Castro, V.F. Ferreira, A.V. Pinto, Naphthoquinoidal [1,2,3]-triazole, a new structural moiety active against *Trypanosoma cruzi*. *Eur. J. Med. Chem.* 43 (2008) 1774-1780.
- [7] P.F. Carneiro, M.C. Pinto, R.K.F. Marra, F.C. da Silva, J.A. Resende, L.F.R. e Silva, H.G. Alves, G.S. Barbosa, M.C. de Vasconcellos, E.S. Lima, A.M. Pohlit, V.F. Ferreira, Synthesis and antimalarial activity of quinones and structurally-related oxirane derivatives, *Eur. J. Med. Chem.* 108 (2016) 134-140.
- [8] L.M. Monteiro, R. Löbenberg, P.C. Cotrim, G.L. Barros de Araujo, N. Bou-Chacra, Buparvaquone Nanostructured Lipid Carrier: Development of an Affordable Delivery System for the Treatment of Leishmaniases. *BioMed Res. Int.* (2017) ID 9781603.
- [9] Y.X. Guo, L. Liu, D.Z. Yan, J.P. Guo, Plumbagin prevents osteoarthritis in human chondrocytes through Nrf-2 activation, *Mol. Med. Rep.* 15 (2017) 2333-2338.
- [10] R.S. Brilhante, E.P. Caetano, R.A. Lima, F.J. Marques, D.S. Castelo-Branco, C.V. Melo, G.M. Guedes, J.S. Oliveira, Z.P. Camargo, J.L. Moreira, A.J. Monteiro, T.J. Bandeira, R.A. Cordeiro, M.F. Rocha, J.J. Sidrim, Terpinen-4-ol, tyrosol, and β -lapachone as potential antifungals against dimorphic fungi, *Braz. J. Microbiol.* 47 (2016) 917-924.
- [11] M. de Barros, P.G. Perciano, M.H. dos Santos, L.L. de Oliveira, E.D. Costa, M.A.S. Moreira, Antibacterial Activity of 7-Epiclusianone and Its Novel Copper Metal

Complex on Streptococcus spp. Isolated from Bovine Mastitis and Their Cytotoxicity in MAC-T Cells, *Molecules* 22 (2017) E823.

[12] M.F. Cardoso, K. Salomão, A.C. Bombaça, D.R. da Rocha, F.C. da Silva, J.A.S. Cavaleiro, S.L. de Castro, V.F. Ferreira, Synthesis and anti-Trypanosoma cruzi activity of new 3-phenylthio-nor- β -lapachone derivatives, *Bioorg. Med. Chem.* 23 (2015) 4763-4768.

[13] R.D. Taylor, M. MacCoss, A.D. Lawson, Rings in Drugs, *J. Med. Chem.* 57 (2014) 5845-5859.

[14] E.N. Silva Júnior, M.A.B.F. Moura, A.V. Pinto, M.C.F.R. Pinto, M.C.B.V. de Souza, A.J. Araújo, C. Pessoa, L.V. Costa-Lotufo, R.C. Montenegro, M.O. de Moraes, V.F. Ferreira, M.O.F. Goulart Cytotoxic, Trypanocidal Activities and Physicochemical Parameters of nor- β -Lapachone-based 1,2,3-Triazoles, *J. Braz. Chem. Soc.* 20 (2009) 635-643.

[15] M.F.C. Cardoso, P.C. Rodrigues, M.E.I.M. Oliveira, I.L. Gama, I.M.C.B. da Silva, I.O. Santos, D.R. Rocha, R.T. Pinho, V.F. Ferreira, M.C.B.V. de Souza, F.C. da Silva, F.P.S. Junior, Synthesis and evaluation of the cytotoxic activity of 1,2-furanonaphthoquinones tethered to 1,2,3-1H-triazoles in myeloid and lymphoid leukemia cell lines, *Eur. J. Med. Chem.* 84 (2014) 708-717.

[16] T. Mosmann, Rapid colorimetric assay for cellular growth and survival: application to proliferation and cytotoxicity assays, *J. Immunol. Methods* 65 (1983) 55-63.

[17] M.C. Alley, D.A. Scudiero, A. Monks, M.L. Hursey, M.J. Czerwinski, D.L. Fine, B.J. Abbott, J.G. Mayo, R.H. Shoemaker, M.R. Boyd, Feasibility of drug screening with panels of human tumor cell lines using a microculture tetrazolium assay, *Cancer Res.* 48 (1988) 589-601.

- [18] International Organization For Standardization. ISO 10993-5. Biological evaluation of medical devices - Part 5: Tests for in vitro cytotoxicity, 24p, 2009.
- [19] M.J. Parnham, H. Wetzig, Toxicity screening of liposomes, *Chem. Phys. Lipids* 64 (1993) 263-274.
- [20] D. Fischer, Y. Li, B. Ahlemeyer, J. Krieglstein, T. Kissel, In vitro cytotoxicity testing of polycations: influence of polymer structure on cell viability and hemolysis, *Biomaterials* 24 (2003) 1121-1131.
- [21] M. Bauer, C. Lautenschlaeger, K. Kempe, L. Tauhardt, U.S. Schubert, D. Fischer, Poly(2-ethyl-2-oxazoline) as alternative for the stealth polymer poly(ethylene glycol): comparison of in vitro cytotoxicity and hemocompatibility, *Macromol. Biosci.* 12 (2012) 986-998.
- [22] A.K. Jordão, V.F. Ferreira, E.S. Lima, M.C.B.V. de Souza, E.C. Carlos, H.C. Castro, Synthesis, antiplatelet and in silico evaluations of novel N-substituted-phenylamino-5-methyl-1H-1,2,3-triazole-4-carbohydrazides. *Bioorg. Med. Chem.* 17 (2009) 3713-3719.
- [23] P.C. Sathler, A.L. Lourenço, C.R. Rodrigues, L.C.R.P. da Silva, L.M. Cabral, A.K. Jordão, A.C. Cunha, M.C.B. Vieira, V.F. Ferreira, C.E. Carvalho-Pinto, H.C. Kang, H.C. Castro. In vitro and in vivo analysis of the antithrombotic and toxicological profile of new antiplatelets N-Acylhydrazone derivatives and development of nanosystems: determination of novel NAH derivatives antiplatelet and nanotechnological approach, *Thromb. Res.* 134 (2014) 376-383.
- [24] J.C. Martinichen-Herrero, E.R. Carbonero, G.L. Sasaki, P.A.J. Gorin, M. Iacomini. Anticoagulant and antithrombotic activities of a chemically sulfated galactoglucomannan obtained from the lichen *cladonia ibitipocae*, *Int. J. Biol. Macromol.* 35 (2005) 97-102.

- [25] B.L. Staker, K. Hjerrild, M.D. Feese, C.A. Behnke, A.B. Burgin, L. Stewart, The mechanism of topoisomerase I poisoning by a camptothecin analog. *Proc. Natl. Acad. Sci. USA* 99 (2002) 15387-15392.
- [26] H. Wei, A.J. Ruthenburg, S.K. Bechis, G.L. Verdine, Nucleotide-dependent Domain Movement in the ATPase Domain of a Human Type IIA DNA Topoisomerase, *J. Biol. Chem.* 280 (2005) 37041-37047.
- [27] C.-C. Wu, T.-K. Li, L. Farh, L.-Y. Lin, T.-S. Lin, Y.-J. Yu, T.-J. Yen, C.-W. Chiang, N.-L. Chan, Structural Basis of Type II Topoisomerase Inhibition by the Anticancer Drug Etoposide, *Science* 333 (2011) 459-462.
- [28] O. Trott, A.J. Olson, AutoDock Vina: improving the speed and accuracy of docking with a new scoring function, efficient optimization, and multithreading, *J. Comput. Chem.* 31 (2010) 455-461.
- [29] N. Boechat, V.F. Ferreira, S.B. Ferreira, M.L.G. Ferreira, F.C. da Silva, M.M. Bastos, M.S. Costa, M.C.S. Lourenço, A.C. Pinto, A.U. Krettli, A.C. Aguiar, B.M. Teixeira, N.V. da Silva, P.R.C. Martins, F.A.F.M. Bezerra, A.L.S. Camilo, G.P. da Silva, C.C.P. Costa, Novel 1,2,3-Triazole Derivatives for Use against *Mycobacterium tuberculosis* H37Rv (ATCC 27294) Strain, *J. Med. Chem.* 54 (2011) 5988-5999.
- [30] I.F. da Silva, P.R.C. Martins, E.G. da Silva, S.B. Ferreira, V.F. Ferreira, K.R.C. da Costa, M.C. de Vasconcellos, E.S. Lima, F.C. da Silva., Synthesis of 1*H*-1,2,3-triazoles and Study of their Antifungal and Cytotoxicity Activities, *Med. Chem.* 9 (2013) 1085-1090.
- [31] S.B. Ferreira, D.T.G. Gonzaga, W.C. Santos, K.G.L. Araujo; V.F. Ferreira, β -Lapachona: Sua importância em química medicinal e modificações estruturais. *Rev. Virtual Quim.* 2 (2010) 140-160.

- [32] M.N. Silva, V.F. Ferreira, M.C.B.V. de Souza, Um Panorama Atual da Química e da Farmacologia a de Naftoquinonas, com Ênfase na beta-Lapachona e Derivados, *Quim. Nova* 26 (2003) 407-416.
- [33] K.W. Wellington, Understanding cancer and the anticancer activities of naphthoquinones - a review, *RSC Adv.* 5 (2015) 20309-20338.
- [34] J.C. Cole, C.W. Murray, J.W.M. Nissink, R.D. Taylor, R. Taylor, Comparing protein-ligand docking programs is difficult. *Proteins* 60 (2005) 325-332.
- [35] M. Kontoyianni, L.M. McClellan, G.S. Sokol, Evaluation of Docking Performance: Comparative Data on Docking Algorithms, *J. Med. Chem.* 47 (2004) 558-565.
- [36] A.R. Leach, B.K. Shoichet, C.E. Peishoff, Prediction of protein-ligand interactions. Docking and scoring: Successes and gaps. *J. Med. Chem.* 49 (2006) 5851-5855.
- [37] B.L. Staker, M.D. Feese, M. Cushman, Y. Pommier, D. Zembower, L. Stewart, A.B. Burgin, Structures of Three Classes of Anticancer Agents Bound to the Human Topoisomerase I–DNA Covalent Complex, *J. Med. Chem.* 48 (2005) 2336-2345.
- [38] C.-C. Wu, Y.-C. Li, Y.-R. Wang, T.-K. Li, N.-L. Chan, On the structural basis and design guidelines for type II topoisomerase-targeting anticancer drugs, *Nucleic Acids Res.* 41 (2013) 10630-10640.
- [39] D. Gurbani, V. Kukshal, J. Laubenthal, A. Kumar, A. Pandey, S. Tripathi, A. Arora, S.K. Jain, R. Ramachandran, D. Anderson, A. Dhawan, Mechanism of Inhibition of the ATPase Domain of Human Topoisomerase II α by 1,4-Benzoquinone, 1,2-Naphthoquinone, 1,4-Naphthoquinone, and 9,10-Phenanthroquinone. *Toxicol. Sci.* 126 (2012) 372-390.

Furanaphthoquinones Tethered to 1H-1,2,3-Triazoles were synthesized

Triazolyl-naphthoquinones have been evaluated against cancer cells

The compounds were tested in MDA-MB231, Caco-2 and Calu-3 human cancer cells

Compound **7a** was the most selective compound on Caco-2 cells

In silico study suggest the blockage of topoisomerase I and II α as mechanism